J. Fluid. Mech. (1985), *vol.* 150, *pp.* 253–280
Printed in Great Britain

The structure of a steady high-speed deflagration with a finite origin

By D. R. KASSOY
Mechanical Engineering Department, University of Colorado, Boulder, Colorado 80309, U.S.A.

AND J. F. CLARKE
Aerodynamics, Cranfield Institute of Technology, Bedford MK43 0AL, England

(Received 11 June 1983 and in revised form 1 August 1984)

A theoretical study is made of the structure of a steady planar deflagration downstream of a specific origin location from which a compressible reactive gas flow emanates. The chemistry is modelled by a high-activation-energy Arrhenius reaction-rate law without the introduction of an ignition temperature. Chemically derived heat addition is significant relative to the initial thermal energy of the flow. Perturbation methods, based on the limit of high activation energy, are used to construct solutions for sub- and supersonic values of the Mach number M at the origin. With the exception of a thin layer adjacent to the origin in which very small changes occur, the structure of the deflagration is determined by a fundamental balance of convection, reaction and compressibility effects. Transport processes have an insignificant effect on the energetics of the flow. The upstream portion of the deflagration is dominated by an ignition event reminiscent of the induction period of an adiabatic thermal explosion. Subsequently in the neighbourhood of a well-defined ignition delay (or explosion) location a very rapid reaction takes place with order-unity changes in all the dependent variables. Compressibility effects are shown to be the source of basic limitations on the maximum temperature rise permitted in a flow with a particular value of M. Chapman–Jouguet deflagrations are found to appear when the chemical heat addition is maximized for a given M. Subsonic combustion is shown to exist for fairly general initial conditions at the origin. In contrast, a purely supersonic reaction is found to be possible only for specifically defined values of the initial strain rate and temperature gradient which would be difficult to control in the experimental environment.

1. Introduction

The structure of an ordinary, steady planar, premixed laminar flame is determined by an interaction between chemical heat release, radical generation and transport-property effects. Conduction and mass diffusion limit the propagation speed to values less than 1 m/s. Faster flames can be achieved by overcoming the limitations of molecular-transport effects. For example, turbulent flame speeds of 10 m/s are possible because velocity and scalar fluctuations enhance the rate at which hot reacting material advances into unburned gas ahead. Even faster combustion waves can be produced if precursor mixing is avoided entirely. The reaction zone in a standing-detonation-wave experiment (Nicholls 1963) propagates at a speed characterized by 10^2 m/s. High temperature behind the normal shock reduces the chemical timescale sufficiently to permit the wave to propagate as a convecting

chain-branching thermal reaction. Neither molecular nor Reynolds-transport mechanisms are required.

Williams (1965) and Buckmaster & Ludford (1982) describe classical and contemporary efforts to model a steady, molecular-transport-dominated flame that propagates at a Mach number characterized by $M = O(10^{-3})$. Both flameholder and doubly infinite models are discussed. Recently Clarke (1983*a*) generalized the former to include larger combustion wave speeds. He demonstrated that the physical mechanism controlling the propagation of the vigorous combustion zone into the unburned mixture changes from molecular transport to convecting chemical reaction as the wave speed increases from $M = O(10^{-3})$ to $M = O(10^{-2})$. Here it is recognized that the wave speed is equal to the prescribed speed at which reactive material is emitted from the origin.

In the present work we consider the structure and physical properties of a steady, planar, compressible combustion wave downstream of a finite origin (flameholder) when the specified wave speed is characterized by $M = O(1)$. We find that important changes in the structural properties of the wave occur with variation in speed and that there is a unique relationship between speed and the gradients at the origin.

Mathematical models for transport-dominated steady planar flames fall into two general categories. The first, exemplified by the study by Bush & Fendell (1970), treats the flame as being embedded in a doubly infinite space. In order to prevent significant consumption of reactants in the semi-infinite region upstream of the reaction zone, the Arrhenius kinetic law is altered so that a zero reaction rate is maintained until the gases reach a specified ignition temperature. As a result, the flame is a transitional structure between upstream and downstream equilibrium states where spatial gradients and chemical rates vanish identically. Only one propagation speed is compatible with a smooth transition from one equilibrium state (zero gradients) to the next. In contrast the propagation speed can be specified for the burner-attached flame model devised by Hirschfelder & Curtiss (1949) and described, for example, by Carrier, Fendell & Bush (1978), Clarke & McIntosh (1980) and by Buckmaster & Ludford (1982). In this case the reactive mixture emanates at a prescribed speed from an origin which is not an equilibrium point. Gradients of temperature, concentration and speed at the origin adjust to the speed so that a steady-state flame exists downstream of the origin. The overall structure varies with flow rate. There is a well-defined range of propagation speeds, for which transport-property-dominated flames exist. At a sufficiently large critical speed, flame separation occurs. The entire transport-dominated flame is located at a distance from the origin which is large compared with the total flame thickness itself (Buckmaster & Ludford 1982, p. 29). Between the origin and the flame the physical processes are dominated by a balance of weak reaction and convection and the gradients are small but finite (Clarke 1983*a*). The subsequent flame is described precisely by the classical doubly infinite model. There is a smooth transition, represented mathematically by formal matching between the upstream small-gradient region and the inert part of the flame itself. In this context, one can recognize that the eigenvalue flame speed, associated with the doubly infinite model, is equal to the critical speed at the origin required to induce separation of an attached flame!

That there is no *a priori* reason to limit inlet speeds in a steady one-dimensional flow can now be appreciated from the work (Clarke 1983*a*,*b*) that shows how the transported-dominated structure gives way first to convection–reaction balances and then to the intervention of compressibility. The stability of these transitional and fast flames must be investigated in due course, but for the present our preoccupation is with the establishing of basic structures.

The doubly infinite space model has also been used to describe flames that propagate at higher speeds than those permitted by classical theory. For example, Kapila, Matkowsky & van Harten (1983) describe a high-activation-energy compressible-flow model in which the propagation Mach number $M = O(1)$ and the heat addition from reaction is vanishingly small relative to the internal energy of the unburned gases. An ignition temperature, thought of as a gas-mixture property, is defined to ensure that the unburned mixture is inert until conduction preheating raises the mixture temperature to the ignition value. The propagation speed M, a function of the ignition temperature, is determined uniquely by the single transitional solution that is compatible with the initial and final equilibrium states. When $M = O(1)$, the ignition temperature must be exceedingly close to the unburned gas temperature far upstream of the reaction zone. It is not known if the ignition temperature can be identified as a true material property, independent of an experimental apparatus.

The Kapila *et al.* model shows that the high-speed flame results from a physical balance of fluid convection, chemical heat release and compressibility effects. Transport-property effects are essentially negligible. In contrast, Stewart & Ludford (1983) have developed a doubly infinite space model for a high-speed reaction zone in which the lengthscale of the entire flame is a modest multiple of the mean free path, and heat release occurs in a thinner, embedded reaction zone dominated by transport effects. The reaction zone is located where the temperature is close to an ignition temperature, which is thought of as a material property of the unburned gas mixture. The flame speed is a unique function of the ignition temperature independent of the detailed reaction process. Implicit in this model is the requirement that the characteristic reaction time is much shorter than the average intermolecular collision time, a condition we believe is difficult to justify on kinetic grounds. As a result, the structural features of this model differ significantly from those of Kapila *et al.* (1983). In particular the extremely short region of active chemical heat release is to be contrasted with an extended zone of compressible reactive flow in the latter work.

High-speed flame structure models are found in early descriptions of one-dimensional idealized detonation waves (Fickett & Davis 1979). For example Duff (1978) describes the structure of a reaction zone (flame), free of transport-property effects and downstream of a shock wave, to show how chain-branching effects cause an induction delay time. Hirschfelder & Curtiss (1958), Linder, Curtiss & Hirschfelder (1958) and Curtiss, Hirschfelder & Barnett (1959) employ the complete reactive Navier–Stokes equations to describe the details of the shock transition as well as the reaction process. In the first of these papers the reaction zone is merged with the shock because it is assumed, arbitrarily, that the characteristic reaction time is short compared with the typical molecular collision time. This result, based of course on a physically implausible assumption, led to a considerable debate in the literature about the importance of transport-property effects in the reaction zone of an idealized detonation wave. Later Wood & Salsburg (1960) and then Adamson (1960), Wood (1961), Koumoutses & Kovitz (1963) and Bowen (1967) showed quite clearly that, for more realistic values of the reaction time, the classical ZND detonation model (see e.g. Williams 1965; for a contemporary application Tarver 1982) composed of an inert shock followed by a reaction zone free of transport effects, was conceptually correct. Perturbation methods were employed in the last four papers to construct solution profiles when the ratio of the collision time to the reaction time is small. Explicit high-activation-energy asymptotics were used by Bush & Fendell (1971) to resolve the structure of a Chapman–Jouguet detonation. Transport effects are confined to the inert shock wave. In contrast, Lu & Ludford (1982) describe a model

of an idealized detonation wave in which most of the heat release occurs in a thin region dominated by conduction and diffusion. This predecessor to the Stewart & Ludford (1983) work is based also on a reaction time short in comparison with the mean interval between collisions. It should be noted that the idealized detonation-wave model, composed of a shock followed by a reaction zone, is unstable in both one and three dimensions (Erpenbeck 1962*a*, 1963, 1964, 1967, 1970). Since a shock alone in a perfect gas is known to be stable (Erpenbeck 1962*b*), the instability of the composite structure must result from an interaction between the shock and disturbances in the exothermic reaction zone itself. The stability of a high-speed reaction zone by itself has not been examined.

Higher-speed flames have also been considered in the context of a flameholder model. Clarke (1983*a*) has described the alteration in structure caused by an increase in the magnitude of the effective propagation speed M. He shows that the transport-dominated structure at $M = O(10^{-3})$ gives way to a convected–reaction structure when $O(10^{-2}) < M \ll 1$. In the latter case each reactive gas particle undergoes an ignition process in the sense of a Semenov-adiabatic thermal explosion (Semenov 1928), which has been discussed in contemporary terms by Kassoy (1975). Gradients at the origin are exponentially small relative to the high activation-energy parameter. This very slight non-equilibrium condition is enough to allow for a wide range of mass-flow rates and hence propagation speeds. It is essential to recognize that Clarke's (1983*a*) model is valid only for $M \ll 1$, so that compressibility effects are ignored.

Clarke (1983*b*) also uses a flameholder configuration to describe the general properties of both sub- and supersonic steady, one-dimensional, compressible reactive flows for a gas with simplified thermodynamic properties and $M = O(1)$. An emphasis is placed on developing a general understanding of the interaction between gas-dynamics, including compressibility, and distributed heat addition due to chemical reaction rather than on calculating the actual reaction-zone structure. (The present paper concentrates specifically on elucidation of these matters.) High-speed reaction-zone propagation is shown to be characterized by convective–reaction effects. Flame sheets, dominated by transport effects, cannot exist because the flow residence time is too short for diffusive effects to smooth out the consequence of chemical reaction. However, transport properties do play a major role in shock transitions downstream of a supersonic flameholder. Shocks are essentially inert because the characteristic chemical reaction time is long relative to the flow passage time through the shock interior. In molecular terms there is insufficient time for reactive collisions to occur.

In the present work we again model the structure of a steady planar deflagration downstream of a specific origin from which a compressible reactive gas flow emanates. One immediate advantage of this formulation is that the reaction process can develop from any chosen initial temperature rather than at an abstractly defined ignition value. The chemical reaction-rate law is of the classical Arrhenius form and includes a large activation energy. At the origin, the gradients and the chemical Reaction rate are exponentially small with respect to the large activation energy. This is compatible with the experimentally required condition that the thermal induction time of the reactive gas in the hypothetical apparatus upstream of the origin be very long compared with the residence time there and with the important chemical scales in the deflagration. If this condition was not met the experimental observation would be of a time-dependent thermal explosion within the apparatus, rather than a steady deflagration downstream of the origin. The finite gradients at the origin, although exceedingly small, permit the degree of freedom necessary to specify the mass-flow rates. In order to model realistic systems the chemical-heat addition is considered

to be significant relative to the initial enthalpy of the reactive gas. This should be contrasted with the small-heat-addition assumption of Kapila *et al.* (1983).

Solution development is by asymptotic expansions based on the high-activation-energy limit. The results obtained are valid for a perfect-gas mixture with fairly general thermodynamic properties. No special assumptions are made about the value of the Prandtl and Lewis numbers.

When M^2 is of order unity and less than $1/\gamma$, where γ is the constant ratio of specific heats, the reaction is initiated in a region where transport effects are important. Its characteristic dimension is a modest multiple of the mean free path, typically 10^{-5} cm for these high-speed flows. Deviations from the initial state are exponentially small with respect to the high-activation-energy limit. Subsequently an ignition process, resembling a convecting thermal explosion, occurs on a much longer lengthscale,† where larger deviations from the initial state exist. The end of the ignition process occurs at a well-defined ignition-delay (or explosion) location in the neighbourhood of which a very rapid reaction process develops. All of the independent variables undergo order-unity changes. This region is characterized by a fundamental coupling between reaction and compressibility effects. The latter are the source of basic restrictions on the maximum temperature rise in the flow for a specified value of M. Sonic speeds downstream of the deflagration (Chapman–Jouguet conditions) are found to be associated with a maximized heat addition for a given M.

For allowable subsonic values of M the downstream combustion process will develop from a wide range of initial velocity gradients at the origin. In contrast, when $M > 1$ a purely supersonic combustion process is possible only for very specifically defined values of the initial strain rate. For all other values of this gradient a shock wave will appear somewhere downstream of the initial location, as described by Clarke (1983*b*). The embedded-shock problem (e.g. the idealized detonation) is not considered here. Suffice it to say that the subsonic combustion fields described here can be matched to the downstream end of any embedded shock as described in the paper just referred to.

2. Mathematical model

In order to develop a rational description of a planar steady high-speed deflagration it is necessary to use the equations describing a compressible, viscous, heat-conducting, diffusing, reactive gas mixture. The general equations discussed by Williams (1965) can be simplified to some extent without diminishing the appropriate representation of the important physical processes. In terms of material properties it is assumed that the species specific heats and binary diffusion coefficients are equal and dependent on the local thermodynamic state. The former condition simplifies the energy equation, while the latter permits Fick's law to be derived from the general equation for the diffusion velocity. The species molecular weights are assumed equal in order to use a perfect-gas equation of state for the mixture. Formally, the chemistry is described by the global decomposition reaction $A \rightarrow B$. However, an identical reaction expression can be derived for a global fuel–oxidizer reaction, $F + O_x \rightarrow$ products, if the initial mixture is either fuel-lean or fuel-rich. The reaction rate is described by the Arrhenius rate law, which contains an exponential dependence on the negative inverse temperature.

The non-dimensional equations for mass and momentum conservation (integrated

† The lengthscale here is very sensitive to local temperature values and may range from unrealistically large values down to wholly realistic values of the order of a centimetre.

once) and for conservation of reactant and energy can be written respectively as

$$\hat{\rho}\hat{u} = 1, \quad \tfrac{4}{3}(\hat{\mu}\hat{u}' - \sigma_1) = \hat{p} + \hat{u} - 1, \tag{1a,b}$$

$$\hat{y}' = \frac{\mathbb{L}}{\mathbb{P}}(\hat{\rho}\hat{D}\hat{y}')' - \left[\frac{B\mu_1}{\gamma p_1 \mathbb{M}^2}\right]\hat{\rho}\hat{y}\, \mathrm{e}^{-1/\epsilon\hat{T}}, \tag{1c}$$

$$\hat{C}_p\hat{T}' = \frac{(\hat{\lambda}\hat{T}')'}{\mathbb{P}} + \left[\frac{B\mu_1}{\gamma p_1 \mathbb{M}^2}\right]h\hat{\rho}\hat{y}\, \mathrm{e}^{-1/\epsilon\hat{T}} + (\gamma - 1)\,\mathbb{M}^2(\hat{u}\hat{p}' + \tfrac{4}{3}\hat{\mu}\hat{u}'^2), \tag{1d}$$

$$\hat{\rho}\hat{T} = 1 + \gamma\mathbb{M}^2\hat{p},$$

where $\hat{\mu}$, $\hat{D}$, $\hat{C}_p$ and $\hat{\lambda}$ are specified functions of T and p at most.

The non-dimensional variables, defined with respect to quantities evaluated at an initial location denoted by the subscript 1, are

$$\left.\begin{aligned} \hat{\rho} &= \frac{\rho}{\rho_1}, \quad \hat{u} = \frac{u}{u_1}, \quad \hat{T} = \frac{T}{T_1}, \quad \hat{p} = \frac{p - p_1}{\rho_1 u_1^2}, \\ \hat{\lambda} &= \frac{\lambda}{\lambda_1}, \quad \hat{D} = \frac{D}{D_1}, \quad \hat{\mu} = \frac{\mu}{\mu_1}, \quad \hat{C}_p = \frac{C_p}{C_{p1}}. \end{aligned}\right\} \tag{2}$$

The reactant mass concentration is denoted by $\hat{y}$. In (1) the primes denote a spatial derivative with respect to the independent variable $\hat{\chi}$, where

$$\hat{\chi} = \frac{\chi}{\chi_{\mathrm{R}}}, \quad \chi_{\mathrm{R}} = \frac{\mu_1}{\rho_1 u_1}. \tag{3}$$

The reference lengthscale χ_{R} is a modest multiple of the mean free molecular path when the initial Mach number $\mathbb{M}$ (see (4) below) is of order unity.

The parameters in (1) are defined by

$$\left.\begin{aligned} \epsilon &= \frac{RT_1}{E}, \quad \mathbb{L} = \frac{\rho_1 D_1 C_{p1}}{\lambda_1} = \frac{\rho_1 D_1 \mathbb{P}}{\mu_1}, \quad \mathbb{P} = \frac{C_{p1}\mu_1}{\lambda_1}, \\ \mathbb{M}^2 &= \frac{u_1^2}{\gamma R T_1}, \quad h = \frac{\Delta H}{C_{p1} T_1}, \quad \sigma_1 = u_1', \quad \gamma = \frac{C_{p1}}{C_{v1}}, \end{aligned}\right\} \tag{4}$$

where R is the gas constant and E is the global activation energy for the reaction considered. The initial Lewis, Prandtl and Mach numbers are given by $\mathbb{L}$, $\mathbb{P}$ and $\mathbb{M}$ respectively. The quantity ΔH is the heat released in the complete consumption of a unit mass of reactant, while σ_1 represents the initial value of the strain rate. Finally the quantity denoted by B in (1c,d) represents the preexponential factor in the Arrhenius rate law.

It should be noted that (1a,b) represent integrated forms of the conservation of mass and momentum considered with respect to the initial location.

A steady planar reaction zone is assumed to exist downstream of a delivery system located at $\hat{\chi} = 0$. The initial conditions are given by

$$\hat{\rho} = \hat{T} = \hat{u} = 1, \quad \hat{p} = 0 \quad \text{at } \hat{\chi} = 0; \tag{5}$$

together with specification of the reactant's fractional mass flux. This implies that the values of the parameters in (4), with the notable exception of σ_1, are known. In particular the initial Mach number $\mathbb{M}$ is to be treated as a finite quantity which may be sub- or supersonic. The flameholder is of the Hirschfelder & Curtiss (1949) type, and so weak upstream diffusion of product is permitted in this formulation. The amount will be calculated in the course of the analysis.

The boundary conditions are completed formally by specifying the downstream pressure, the condition for completion of the reaction process and the approach to a final equilibrium state:

$$\hat{p} = \hat{p}_\infty, \quad \hat{y} = 0, \quad (\ )' = 0 \quad \text{as } \hat{\chi} \to \infty. \tag{6}$$

The last expression implies that the dependent-variable derivatives must approach zero far from the initial point.

The flameholder configuration implied by (5) and (6) is employed to emulate the experimental environment. There, the prudent observer must prevent spontaneous ignition of the reactive mixture prior to the exit of the delivery system by making the thermal ignition time of the mixture much larger than the system residence time. This can be accomplished by specifying a high mass-flow rate, by choosing a delivery system with a small lengthscale, by operating at a low system temperature, or a suitable combination of the three effects. For example a cold reactive mixture could be passed through a supersonic nozzle and then be compressed and heated by a normal exit shock. The shock strength would be chosen to provide the nearly instantaneous temperature boost required to ensure that a significant reaction occurs subsequent to the shock. The state just downstream of the shock location would provide the initial conditions in (5) in the case of $\mathcal{M} < 1$. The standing-detonation-wave experiments of Nicholls (1963) provide an example of this type of experiment. Alternatively one could mix cold reactants and pass them very quickly through a cooled flameholder such that the exit temperature was sufficiently high to ensure a subsequent reaction process. Then the exit conditions provide the initial state in (5).

The flameholder model used here does not require the definition of an arbitrary ignition temperature used often in infinite-field flame models to initiate the reaction at a specified finite location (Bush & Fendell 1970). In the same sense the classical cold-wall boundary difficulty (Williams 1965) is avoided.

The two-point boundary-value problem defined by (1), (5) and (6) is awkward for the development of solution trajectories for each variable from the initial to the final state. In this sense it is advantageous to convert the problem to an initial-value type by establishing a relationship between $\hat{p}_\infty$ and the initial strain rate σ_1. If (1*c*,*d*) are integrated between the initial and final states and (1*a*,*e*) are evaluated for $\hat{\chi} \to \infty$ it then follows that

$$-\tfrac{4}{3}\sigma_1 = \hat{p}_\infty + \hat{u}_\infty - 1, \tag{7a}$$

$$\hat{y}(0) = \frac{\mathbb{L}}{\mathbb{P}}\hat{y}'(0) + \left[\frac{B\mu_1}{\gamma p_1 \mathcal{M}^2}\right]\int_0^\infty \hat{\rho}\hat{y}\, \mathrm{e}^{-1/\epsilon\hat{T}}\, \mathrm{d}\hat{\chi}, \tag{7b}$$

$$\int_1^{\hat{T}_\infty} \hat{C}_p\, \mathrm{d}\hat{T} = \frac{-1}{\mathbb{P}}\hat{T}'(0) + h\left(\hat{y}(0) - \frac{\mathbb{L}}{\mathbb{P}}\hat{y}'(0)\right) - (\gamma - 1)\mathcal{M}^2\left(\tfrac{1}{2}(\hat{u}_\infty^2 - 1) + \tfrac{4}{3}\sigma_1\right), \tag{7c}$$

$$\hat{T}_\infty = \hat{u}_\infty(1 + \gamma\mathcal{M}^2\hat{p}_\infty). \tag{7d}$$

There are four independent equations in (7) for the seven unknowns $\hat{u}_\infty$, $\hat{T}_\infty$, $\hat{\sigma}_1$, $\hat{y}(0)$, $\hat{y}'(0)$, $\hat{T}'(0)$ and the integral in (7*b*). If the structural solution can be shown to yield information about the derivatives $\hat{y}'(0)$, $\hat{T}'(0)$ and the value of the integral, then the remaining unknowns can be evaluated. This will be validated in §3. It follows that a specification of $\hat{p}_\infty$ implies σ_1 and *vice versa*. It should be noted that (7*b*) is used ultimately to calculate $\hat{y}(0)$.

The solution to (1) subject to (5) and $\hat{u}'(0) = \sigma_1$ specified, is to be found when the initial Mach number is finite ($\mathcal{M} = O(1)$) and the initial Lewis and Prandtl numbers are arbitrary but finite. The activation-energy parameter ϵ is considered to be very

small, with values between 0.02 and 0.05 of physical interest. In contrast with Kapila *et al.* (1983) the non-dimensional heat-addition parameter $h = O(1)$, which will permit the kind of heat-addition effects seen in real reactive systems.

The parameter multiplying the reaction terms in (1*c*,*d*) contains the factor μ_1/p_1 proportional to the mean molecular collision interval for the initial state, which is of the magnitude 10^{-10} s for standard temperature and pressure values. Typically the preexponential factor $B = O(10^m\ \mathrm{s}^{-1})$ for $m = O(10)$ (Bradley 1962). Given that $\gamma = O(1)$ and $\mathcal{M} = O(1)$ in addition, it is necessary to treat the quantity $B\mu_1/\gamma p_1 \mathcal{M}^2$ as a number which may be large with respect to the limit $\epsilon \to 0$.

The viscous lengthscale χ_R defined in (3) is of magnitude 10^{-5} cm for standard conditions. This is in fact the thickness of a moderately strong shock corresponding to a mass flux $\rho_1 u_1$ commensurate with $\mathcal{M} = O(1) > 1$. In this regard it should be noted that the initial dimensional strain rate, found from (2)–(4), can be written as

$$\frac{\mathrm{d}u}{\mathrm{d}\chi}(0) = \frac{\gamma \mathcal{M}^2}{\mu_1/p_1}\sigma_1.$$

When $\sigma_1 = O(1)$ the remaining large parameter gives the characteristic strain in a shock. Only if $\sigma_1 \ll O(1)$ will less severe initial strains be present.

Solutions to (1) are to be found in the limit $\epsilon \to 0$ for subsonic initial conditions, $0 < \mathcal{M} < 1$, and in the supersonic case $\mathcal{M} > 1$ when the flow is shock-free. In either case it is assumed that $\sigma_1 \ll O(1)$, so that a shock may not exist even at the initial boundary. The supersonic study is carried out explicitly to show that such flows are not likely to be observed.

Embedded shocks, precluded by the conditions prescribed above in the present work, have been considered by Clarke (1983*b*). He shows that behind all such shocks the conditions are those of a subsonic flow with a well-defined σ_1 of a suitably small size. Thus the $\mathcal{M} < 1$ solutions developed here can be matched onto the appropriate downstream solution for the shock (Courant & Friedrichs 1948). Examples of this kind of calculation have been given by Bowen (1967), Bush & Fendell (1971) and Kapila *et al.* (1983).

3. Reaction initiation

The reaction process is to be initiated in the very thin zone, where $\hat{\chi} = O(1)$. There, in the limit $\epsilon \to 0$ the reaction terms in (1*c*,*d*) are exponentially small given that the parameter $B\mu_1/p_1 \mathcal{M}^2$ is not too large. Furthermore the absence of a shock means that σ_1 and hence $\hat{u}'$ are very small. As a consequence changes from the initial state will be minute. The magnitude of the variation is determined by using the asymptotic transformation

$$(\hat{T}, \hat{y}) \sim 1 + \beta(\epsilon)\{\hat{\theta}(\hat{\chi};\epsilon),\ -\hat{c}(\hat{\chi};\epsilon)\},\quad \lim_{\epsilon \to 0} \beta = 0 \tag{8}$$

in (1*c*,*d*) to find equations for the lowest-order approximation to the perturbation quantities $\hat{\theta}$ and $\hat{c}$. These variables will be affected by the weak reaction process only if

$$\beta = \frac{B\mu_1\, \mathrm{e}^{-1/\epsilon}}{\gamma p_1 \mathcal{M}^2} \ll 1. \tag{9}$$

This parameter is observed to be the ratio of the initial mean time between molecular collisions to the reaction time at T_1 when $\mathcal{M} = O(1)$. A more specific limitation must

await further solution development. Gasdynamical effects described by the last term in (1*d*) will be of the same order of magnitude as the reactive term if

$$\hat{p} \sim \beta \hat{P}(\hat{\chi}; \epsilon), \quad \hat{u} \sim 1 + \beta \hat{U}(\hat{\chi}; \epsilon). \tag{10a,b}$$

The latter representation implies that

$$\sigma_1 = \beta \hat{\sigma}_1, \quad \hat{\sigma}_1 \equiv \hat{U}'(0) = O(1). \tag{11}$$

It follows from (1*a–d*) and the limit $\epsilon \to 0$ that the lowest-order approximation for the perturbation quantities can be described by

$$\hat{c}' = \frac{\mathbb{L}}{\mathbb{P}} \hat{c}'' + 1, \quad \hat{c}(0) = \hat{C}_0, \tag{12a}$$

$$\hat{\theta}' = \frac{1}{\mathbb{P}} \hat{\theta}'' + h + (\gamma - 1) M^2 \hat{P}', \quad \hat{\theta}(0) = \hat{P}(0) = 0, \tag{12b}$$

$$\hat{P} = (\hat{\theta} - \hat{U})/\gamma M^2, \tag{12c}$$

$$\tfrac{4}{3}(\hat{U}' - \hat{\sigma}_1) = \hat{P} + \hat{U}, \quad \hat{U}(0) = 0, \tag{12d}$$

where $\hat{\sigma}_1$ is treated as a known initial value and $\hat{C}_0$ is a constant. In deriving the asymptotic approximation to the exponential terms in (1*c*,*d*) it is necessary to assert that $(\beta/\epsilon)\hat{\theta} \ll O(1)$. Given β in (9), this condition will fail to be true only when $\hat{\theta}$ is quite large. In the usual sense, the failure of the limitation on the size of $\hat{\theta}$ will signal the non-uniformity of the solution in the $\hat{\chi}$ region.

Before proceeding with the development of solutions to (12) it is necessary to point out the consequences of a larger initial strain rate. When

$$O(\beta) \ll \sigma_1 \leqslant O(\epsilon)$$

it can be shown that the gasdynamical term in (1*d*) is larger than the chemical term. As a result a basically inert gasdynamical relaxation zone precedes any reaction process. The dependent variables spontaneously approach a new near-equilibrium state downstream (i.e. $\hat{\chi} \to \infty$). When the gradients become $O(\beta(\epsilon))$ the reaction-dominated analysis described above can be implemented. The only effect of larger σ_1 values is to displace the weak reaction downstream by a dimensional distance $O(\chi_R \ln(\sigma_1/\beta))$. The appropriate initial conditions for the reaction zone are given by the downstream equilibrium solution to the inert problem. It should be noted that the upper bound on the magnitude of σ_1 arises from the high activation-energy asymptotics in which temperature perturbations from an initial state will be at most $O(\epsilon)$. Values in the range $O(\epsilon) < \sigma_1 \leqslant O(1)$ imply shock-like processes in which $O(1)$ changes in temperature occur.

Equations (12) can be used to find

$$\left.\begin{aligned} a\hat{\theta}'' + b\hat{\theta}' - (1 - M^2)\hat{\theta} &= -m - n\hat{\chi}, \quad \hat{\theta}(0) = 0, \\ a &= \frac{\frac{4}{3}\gamma M^2}{\mathbb{P}}, \quad b = (1 - \gamma M^2)\mathbb{P} - \tfrac{4}{3}M^2, \\ m &= \tfrac{4}{3}\gamma M^2 h - \frac{\hat{\theta}'(0)}{\mathbb{P}}(1 - \gamma M^2) - \tfrac{4}{3}(\gamma - 1) M^2 \hat{\sigma}_1, \\ n &= h(1 - \gamma M^2), \end{aligned}\right\} \tag{13}$$

where the presence of $\hat{\theta}'(0)$ results from using the integral of (12*b*) relative to the initial point.

3.1. *Subsonic results*

In the case of a subsonic entry condition $\mathcal{M} < 1$ the general solution can be written as

$$\left.\begin{aligned} \theta &= K_1 \, \mathrm{e}^{\lambda_1^2 \hat{\chi}} + K_2 \, \mathrm{e}^{-\lambda_2^2 \hat{\chi}} + R\hat{\chi} + Q, \\ R &= \frac{(1-\gamma\mathcal{M}^2)\, h}{1-\mathcal{M}^2}, \quad Q = \frac{bR+m}{1-\mathcal{M}^2}, \end{aligned}\right\} \tag{14}$$

where λ_1^2 ($-\lambda_2^2$) corresponds to the positive (negative) root of the characteristic equation of the homogeneous operator in (13),

$$\frac{b}{2a}\left\{\pm\left[1+4\frac{(1-\mathcal{M}^2)\, a}{b^2}\right]^{\frac{1}{2}}-1\right\}. \tag{15}$$

The exponential growth of $\hat{\theta}$ in (14) must be suppressed because there is no physical mechanism other than the weak chemistry (represented by the nonhomogeneous terms in (13)) that can produce a temperature rise. If, in addition, the initial condition in (13) is satisfied then the solution can be written as

$$\hat{\theta} = Q(1-\mathrm{e}^{-\lambda_2^2 \hat{\chi}}) + R\hat{\chi}. \tag{16}$$

At $\hat{\chi} = 0$ the initial gradient of the temperature perturbation can be written as

$$\hat{\theta}'(0) = Q\lambda_2^2 + R. \tag{17}$$

Given the definitions of these quantities in (13)–(15), it is clear that (17) provides an explicit value of $\hat{\theta}'(0)$ as a function of $\mathcal{M}$, $\mathbb{P}$, γ, h and $\hat{\sigma}_1$. It follows that, once σ_1 is specified, the heat flux at the origin can be calculated explicitly from $\hat{T}'(0) \sim \beta\hat{\theta}'(0)$ as obtained from (8). It is then clear that the conductive heat loss to the delivery system is $O(\beta)$ for $\mathcal{M}^2 = O(1)$ in this subsonic case.

The fuel-consumption equation (12*a*) has the elementary solution $\hat{c} = \hat{\chi}$, which is obtained by suppressing the exponentially growing homogeneous solution. The result is interpreted to mean that fuel is consumed only by the weak reaction represented by the nonhomogeneous term in (12*a*). At the initial point the reactant gradient found from (8), namely $\hat{y}'(0) \sim -\beta(\epsilon)$, is of course small.

The known values of $\hat{T}'(0)$ and $\hat{y}'(0)$ can now be used in (7*a*, *c*, *d*) so that the system provides three equations for σ_1, $\hat{T}_\infty$, $\hat{u}_\infty$ in the case when $\hat{p}_\infty$ is prescribed. This then verifies the ($\hat{p}_\infty$, σ_1)-relationship implied previously.

The integrated form of (12*b*) can be used to find the pressure perturbation

$$(\gamma-1)\,\mathcal{M}^2\hat{P} = \hat{\theta} - \frac{1}{\mathbb{P}}(\hat{\theta}' - \hat{\theta}'(0)) - h\hat{\chi}, \tag{18}$$

while the speed variation is obtained from (12*c*) in the form

$$\hat{U} = \hat{\theta} - \gamma\mathcal{M}^2\hat{P}. \tag{19}$$

3.2. *Supersonic results*

When $\mathcal{M} > 1$ both roots in (15) are positive. The general solution, analogous to (14), then contains two exponentially growing terms. If the flow is to be purely supersonic there is no mechanism (e.g. a nearby downstream shock) to support these rapid variations. Thus the exponential growth must be suppressed, so that the solution is simply

$$\hat{\theta} = R\hat{\chi} + Q. \tag{20}$$

A fuller discussion of the role of exponential terms is given by Clarke (1983*b*). If the initial condition $\hat{\theta}(0) = 0$ is satisfied, then $Q = 0$, which, after suitable manipulation of the Q-definition in (14), yields

$$\hat{\sigma}_1 = -h/(M^2 - 1). \tag{21}$$

This result shows that a supersonic flow with heat addition ($h \neq 0$) cannot develop from an equilibrium initial state ($\hat{\sigma}_1 \equiv 0$). The flow will remain purely supersonic in the $\hat{\chi} = O(1)$ region only if the initial strain is controlled very precisely. Any deviation from this special value will lead to the presence of a shock just downstream of the initial point, as discussed in detail by Clarke (1983*b*). It should be emphasized that the result given in (21) represents only a lowest-order approximation. If a higher-order theory were developed, small corrections could be calculated. The initial conditions required for a supersonic reaction process would then be even more stringent. All of this suggests that planar purely supersonic combustion cannot be observed experimentally, because of the impossibility of controlling the initial strain rate or pressure difference $p_\infty - p_1$ adequately.

One can use (8) and (20) to show that the initial heat flux is $\hat{T}'(0) \sim \beta\hat{h}$. The pressure and speed perturbations are given by (18) and (19).

3.3. *Asymptotic behaviour and singularities*

The reaction-initiation solutions contain a simple singularity in the limit $\hat{\chi} \to \infty$. From (8), (10), (16) and (18)–(20) it can be shown that to lowest order

$$\hat{y}(\hat{\chi} \to \infty) \sim 1 - \beta(\hat{\chi} + O(\hat{\chi}^0)), \tag{22a}$$

$$\hat{T}(\hat{\chi} \to \infty) \sim 1 + \beta(R\hat{\chi} + O(\hat{\chi}^0)), \tag{22b}$$

$$\hat{p}(\hat{\chi} \to \infty) \sim \beta\left(-\frac{h\hat{\chi}}{1 - M^2} + O(\hat{\chi}^0)\right), \tag{22c}$$

$$\hat{u}(\hat{\chi} \to \infty) \sim 1 + \beta\left(\frac{h\hat{\chi}}{1 - M^2} + O(\hat{\chi}^0)\right). \tag{22d}$$

First it should be noted that given the definition of R in (14) the temperature will increase if $0 < M^2 < 1/\gamma$ or $M^2 > 1$ but will decline for $1/\gamma < M^2 < 1$. In the latter case the decline is proportional to the heat-addition parameter h, implying that the flow converts energy added to the system to kinetic energy in an efficient manner.

The results for the speed and pressure show that in a subsonic (supersonic) flow the pressure drops (increases) as the speed increases (decreases). These results are what one would expect for one-dimensional flow with heat addition (Shapiro 1954).

The approximations inherent in the derivation of (12) fail when

$$(\beta/\epsilon)\,\hat{\theta} \sim (\beta/\epsilon)\,\hat{\chi} = O(1).$$

When $\hat{\chi} = O(\epsilon/\beta)$ it follows that $\hat{y} \sim 1 - O(\epsilon)$, $\hat{T} \sim 1 + O(\epsilon)$, $\hat{p} = O(\epsilon)$ and $\hat{u} \sim 1 + O(\epsilon)$. These estimates are used to determine the scaling in the next region downstream.

It should be noted that $O(\hat{\chi}^0)$ terms in (22*b–d*) contain the factor Q, defined in (14), which depends explicitly on $\hat{\sigma}_1$. This means that when the non-uniformity occurs ($\beta\hat{\chi} = O(\epsilon)$), because heat addition h begins to dominate the process, the influence of transport properties remains $O(\beta)$. As a result the chemical effects begin to decouple from the transport effects at the end of the reaction-initiation period. This decoupling is a characteristic feature of high-speed flows with chemical-energy release (Clarke 1983*a*,*b*).

It is interesting to note that the residence time of a fluid particle in the initiation zone is given by $\chi_R/u_1 = \mu_1/\gamma p_1 M^2$. When the initial Mach number is not too large, the residence time may be considerably larger than the mean interval between collisions, given by μ_1/p_1. This condition is necessary in any quantitatively accurate continuum description of a gasdynamic process.

4. Ignition process

In §3 the reaction initiation was characterized by an inherent balance of convection, conduction and compressibility effects, with heat addition from a relatively weak reaction. Except for $\gamma^{-1} < M^2 < 1$ the cumulative effect of heat addition over the $\hat{\chi}$-region is a rise in gas temperature sufficient to enhance the reaction rate relative to energy transport by conduction. This suggests that in the subsequent region account must be taken of a rather more substantial reaction process.

One may infer from the discussion in §3.3 that the ignition-zone variables can be written as

$$(\hat{T}, \hat{y}, \hat{u}) \sim 1 + \epsilon(\bar{\theta}, -\bar{c}, \bar{U}), \tag{23a}$$

$$\hat{p} \sim \epsilon \bar{P}, \tag{23b}$$

where the perturbation quantities are functions of the stretched coordinate

$$\hat{\chi} = (\epsilon/\beta)\,\bar{\chi} \tag{23c}$$

and the parameter ϵ. The lowest-order matching conditions constructed from (8), (10) and (23) are

$$\bar{\theta} = \bar{c} = \bar{U} = \bar{P} = 0 \quad \text{as } \bar{\chi} \to 0. \tag{24}$$

If (23) is used in (1) the lowest-order approximation in the limit $\epsilon \to 0$, $\bar{\chi}$ fixed, can be written as

$$U = -\bar{P}, \quad \bar{U} = \bar{\theta} - \gamma M^2 \bar{P}, \tag{25a,b}$$

$$\bar{c}' = e^{\bar{\theta}}, \quad \bar{\theta}' = h\, e^{\bar{\theta}} + (\gamma - 1) M^2 \bar{P}', \tag{25c,d,}$$

where primes denote derivatives with respect to $\bar{\chi}$. Equations (25a,c,d), representing conservation of momentum, reactant and energy respectively, are observed to be independent of transport effects. The energy equation exhibits an explicit balance of convection, reaction and compressibility. Equations (25a,b,d) can be rearranged to show that

$$\bar{\theta}' = R\, e^{\bar{\theta}}. \tag{26}$$

The temperature-perturbation solution, subject to (24), is

$$\bar{\theta} = \ln \frac{1}{1 - R\bar{\chi}}. \tag{27}$$

The remaining solutions then take the form

$$\bar{c} = \frac{\bar{\theta}}{R}, \quad \bar{P} = -\frac{\bar{\theta}}{1 - \gamma M^2} = -\bar{U}. \tag{28}$$

If the pressure gradient is evaluated explicitly from (27) and (28) and then used to calculate the value of the compressibility term in (25d), it can be seen that the latter is a heat sink for $M < 1$ and a heat source for $M > 1$. This fact helps to explain the change in character of the $\bar{\theta}$-solution at large subsonic values of M as portrayed qualitatively in figure 1. When $R > 0$, corresponding to $0 < M^2 < 1/\gamma$ and $M^2 > 1$, the solution approaches a positive infinity at a finite location $\bar{\chi}_i = 1/R$. In contrast when $1/\gamma < M^2 < 1$, $R < 0$, the temperature perturbation decreases monotonically

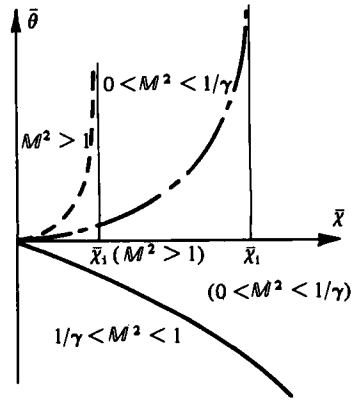

FIGURE 1

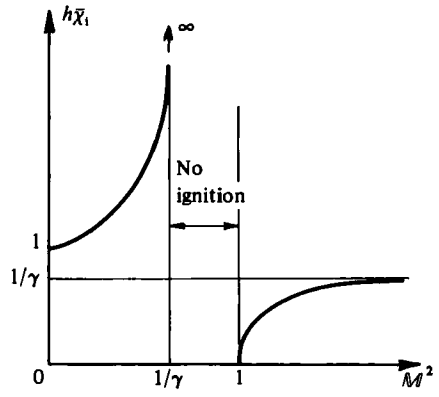

FIGURE 2

FIGURE 1. Temperature-perturbation variation with downstream distance for three Mach-number regimes.

FIGURE 2. The ignition delay distance $h\bar{\chi}_i$ as a function of M^2.

in the $\bar{\chi}$-region, approaching negative infinity for $\bar{\chi}\to\infty$. This occurs because the compressibility heat sink is larger than the reaction-generated heat addition when M^2 is in the critical regime. In this sense the combustion process is subcritical for $1/\gamma < M^2 < 1$ and supercritical for other values of M^2.

The singularity in $\bar{\theta}$ when $R > 0$ is typical of those found in the induction or ignition period of an adiabatic thermal explosion (Kassoy 1975) and has been seen in non-classical flame studies (Clarke 1983*b*; Kapila *et al.* 1983). In figure 2 the ignition-delay distance $h\bar{\chi}_i$ is shown as a function of M^2 for $\gamma = 1.4$. In the range of $0 < M^2 < 1/\gamma$, $\bar{\chi}_i$ increases with M^2 (for a fixed h) as the heat-sink effect of compressibility grows. When $M^2\to(1/\gamma)-$, $h\bar{\chi}_i\to\infty$, implying that the ignition process is delayed indefinitely. In the supersonic regime the heat-source effect of compressibility is very large for $M^2\to 1+$, which causes $h\bar{\chi}_i\to 0$. Further increases in M^2 cause $h\bar{\chi}_i$ to increase at most to $1/\gamma$ because the heat-source effect becomes vanishingly small for large M. It should also be noted that for a given M the value of $\bar{\chi}_i$ decreases with increasing h, implying that ignition appears closer to the initial point when the heat release is larger.

The dimensional ignition-delay distance

$$\chi_i = \frac{\epsilon}{\beta}\bar{\chi}_i\,\chi_R \tag{29}$$

is $O(\epsilon)$ smaller than the distance travelled by a fluid particle at the initial speed u_1 during the initial characteristic reaction-time interval $B^{-1}\,e^{1/\epsilon}$, given the definition of β in (9). Order-of-magnitude estimates for β are given in table 1 for

$$\mu_1/p_1 = O(10^{-10}\text{ s}),\quad \epsilon = O(10^{-2})\quad\text{and}\quad 10^{10}\text{ s}^{-1}\leqslant B\leqslant 10^{20}\text{ s}^{-1}.$$

Generally $\beta \ll O(\epsilon)$ unless ϵ and B are fairly large, corresponding to very large reaction rates. If the typical value $\chi_R = O(10^{-5}\text{ cm})$ is considered, then a laboratory-size ignition-delay distance, say $\chi_i \lesssim 10^3$ cm, can be calculated from (29) only for a subset of β-values in table 1 characterized by $O(10^{-10}) \lesssim \beta \ll O(10^{-2})$, a significant range nonetheless.

In the subsonic, supercritical regime the temperature rise described by (27) is

	$M^2 = O(1)$			$M^2 = O(10^{-2})$		
B ...	10^{10}	10^{15}	10^{20}	10^{10}	10^{15}	10^{20}
ϵ	β	β	β	β	β	β
0.02	2×10^{-22}	2×10^{-17}	2×10^{-12}	2×10^{-20}	2×10^{-15}	2×10^{-10}
0.03	5×10^{-15}	5×10^{-10}	5×10^{-5}	5×10^{-13}	5×10^{-8}	5×10^{-3}
0.04	1×10^{-11}	1×10^{-6}	1×10^{-1}	1×10^{-9}	1×10^{-4}	1×10^{1}
0.05	2×10^{-9}	2×10^{-4}	2×10^{1}	2×10^{-7}	2×10^{-2}	2×10^{3}

TABLE 1. Order-of-magnitude estimates for the parameter β as a function of ϵ when $M^2 = O(1)$ and $M^2 = O(10^{-2})$ for three values of the preexponential factor B

accompanied by a pressure drop and flow acceleration given by (28). In the analogous supersonic flow the pressure rises as the flow is decelerated. The subsonic subcritical regime is characterized by a pressure drop and flow acceleration along with the decline in temperature. The latter effect leads to a monotonic decrease in the reaction rate. In this sense the reaction event, benign in character, must extend over distances which are extraordinarily long relative to a laboratory scale. No further consideration will be given to this case.

The non-uniformity developing in (23) due to the singularities in (27) and (28) when $\bar{\chi}R \to 1-$ is directly related to those seen in thermal explosion theory. In particular one must now develop a procedure for studying $O(1)$-variations in the dependent variables $(\hat{T}, \hat{y}, \hat{u}, \hat{p})$ caused in this problem by a combination of significant heat addition ($h = O(1)$) and gasdynamical processes.

5. Rapid combustion

The perturbations in the ignition zone, formally $O(\epsilon)$, become very large when $\bar{\chi} \to \bar{\chi}_1$ in the sense that $\epsilon \ln(1 - R\bar{\chi}) = O(1)$. This type of non-uniformity is reminiscent of that seen so frequently at the end of the induction period of a thermal explosion (Kassoy 1975). In the region to follow, where it is expected that $O(1)$ changes in the dependent variables will occur, the spatial scaling is defined in terms of a nonlinear transformation relative to the rapidly varying temperature

$$\bar{\chi} = \bar{\chi}_1 - H(\hat{T}; \epsilon) \exp\left\{-\frac{1}{\epsilon}\left[1 - \frac{1}{\hat{T}}\right]\right\}, \tag{30}$$

where $\bar{\chi}_1$ and H can be represented formally by limit-process expansions for $\epsilon \to 0$. The previously defined value $\bar{\chi}_1 = 1/R$ is the lowest-order approximation to the former quantity. If (30) is used in (1 d) the energy equation can be written in the form

$$\hat{C}_p = \frac{\beta}{\hat{p}} \frac{\mathrm{d}}{\mathrm{d}\hat{T}}\left\{\hat{\lambda}\left[\frac{H}{\hat{T}^2} - \epsilon H'\right]^{-1} \exp\left[\frac{1}{\epsilon}\left(1 - \frac{1}{\hat{T}}\right)\right]\right\} + h\hat{\rho}\hat{y}\left[\frac{H}{\hat{T}^2} - cH'\right]$$
$$+ (\gamma - 1) M^2 \left\{\hat{u}\frac{\mathrm{d}\hat{p}}{\mathrm{d}\hat{T}} + \tfrac{4}{3}\beta(\hat{u}')^2\left[\frac{H}{\hat{T}^2} - \epsilon H'\right]^{-1} \exp\left[\frac{1}{\epsilon}\left(1 - \frac{1}{\hat{T}}\right)\right]\right\}. \tag{31}$$

Primes denote derivatives with respect to $\hat{T}$. The limiting form of (31) is sensitive to conditions placed on the parameter β. The magnitude of the conduction and

dissipation terms in (31) (respectively first and fourth on the right-hand side), is determined by the properties of the parameter

$$\beta \exp\left[\frac{1}{\epsilon}\left(1-\frac{1}{\hat{T}}\right)\right] < \beta \exp\left[\frac{1}{\epsilon}\left(1-\frac{1}{\hat{T}^*}\right)\right], \tag{32}$$

where $\hat{T}^* \geqslant T$, the maximum temperature encountered in the rapid-combustion zone, must be found in the course of analysis. One can use (9) in the second term in (32) to show that the latter is nothing more than the ratio of the intermolecular collision time to the characteristic reaction time at the temperature $\hat{T}^*$. In a physically realistic system this ratio must be very small because substantial reaction progress requires many molecular collisions. It follows that

$$\beta \exp\left[\frac{1}{\epsilon}\left(1-\frac{1}{\hat{T}^*}\right)\right] \ll O(1) \tag{33}$$

when $\epsilon \ll 1$. In the limit $\epsilon \to 0$, β must be exponentially small, which sets the magnitude of the perturbations in the initiation zone. The inequality in (33) implies that conduction and dissipation are suppressed in the limiting form of (31) which describes energy transport as a balance of convection, heat addition and compressibility.

It is perhaps worth while to recall that the mean molecular-collision time is related directly to the flow passage time of a gas through all but very weak shock waves (Landau & Lifshitz 1959). In this sense the present study is limited to reactions with timescales that are relatively long compared with the shock flow passage time. This notion is of significance when the deflagration results are applied to reaction zones behind shock waves. In fact Adamson (1960), Wood (1961) and Bowen (1967) invoked these conditions, and that in (33), in their analyses of the idealized detonation wave! Of course for larger β-values one could consider merged shock–reaction zones, particularly for broad weak shocks, although that is not done here. A numerical computation for the merged system has been discussed by Hirschfelder & Curtiss (1958).

Matching conditions for the dependent variables can be constructed from (23), (27), (28) and (30), in terms of $T \to 1+$. These intuitively obvious results are

$$(\hat{y}, \hat{u}) \to 1, \quad \hat{p} \to 0 \quad \text{as } \hat{T} \to 1. \tag{34a}$$

In addition

$$H \to \bar{\chi}_t \quad \text{as } \hat{T} \to 1. \tag{34b}$$

The species and momentum equations in (1) can be transformed using (30) into a form related to that in (31). If the limitation in (33) is applied when $\epsilon \to 0$, $\hat{y} \gg O(\epsilon)$ and $\epsilon H' \gg O(H)$, then the lowest-order approximate equations

$$H(\hat{T}) = [\hat{C}_p + \tfrac{1}{2}(\gamma-1)\,\mathcal{M}^2\,(\hat{u}^2)']\frac{\hat{T}^2\hat{u}}{h\hat{y}}, \tag{35a}$$

$$\hat{y}' = -\hat{\rho}\hat{y}H/\hat{T}^2, \tag{35b}$$

$$\hat{\rho}\hat{u} = 1, \quad \hat{u} = 1-\hat{p}, \quad \hat{\rho}\hat{T} = 1+\gamma\mathcal{M}^2\hat{p} \tag{35c,d,e}$$

represent conservation of energy, species, mass and momentum and the equation of state. Equations (35a,b) can be combined to produce an elementary differential equation for $\hat{y}'$. The solution

$$h\hat{y} = h - \int_1^{\hat{T}} \hat{C}_p(\sigma)\,\mathrm{d}\sigma - \tfrac{1}{2}(\gamma-1)\,\mathcal{M}^2(\hat{u}^2-1) \tag{36}$$

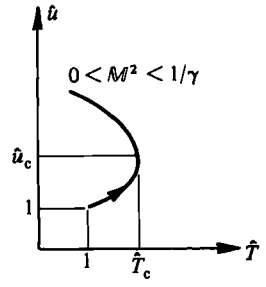

FIGURE 3

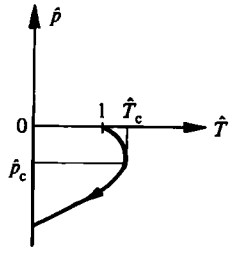

FIGURE 4

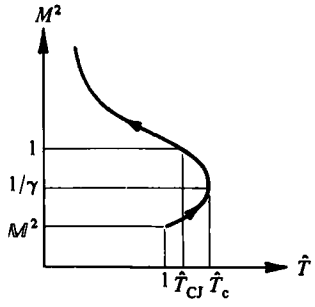

FIGURE 5

FIGURE 3. Flow speed as a function of temperature.

FIGURE 4. Pressure difference as a function of temperature.

FIGURE 5. M^2 as a function of temperature.

satisfies the matching conditions in (34). The algebraic system in (35*c–e*) can be used to show that

$$\left.\begin{aligned} \hat{u}(\hat{T}) &= \frac{1+\gamma M^2}{2\gamma M^2}\left\{1 \mp \frac{1-\gamma M^2}{1+\gamma M^2}[1-\alpha(\hat{T}-1)]^{\frac{1}{2}}\right\}, \\ \alpha &= 4\gamma M^2/(1-\gamma M^2)^2. \end{aligned}\right\} \tag{37}$$

Formally (37) and its derivative can be employed in (35*a*,*b*) to find an explicit expression for $H(\hat{T})$. Similarly $\hat{\rho}, \hat{u}, \hat{p}$ and $\hat{y}$ can be found as functions of $\hat{T}$. Finally $\hat{T} = \hat{T}(\bar{\chi}; \epsilon)$ can be found in implicit form from (30). It should be noted that the solution in (37) is multivalued and must be used judiciously to describe supercritical subsonic and supersonic events.

In the discussion to follow the special case $\hat{C}_p = 1$ is examined in detail. It should be clear that the variable-specific-heat problem can be examined with only a minor increase in algebraic effort.

5.1. *Subsonic initial conditions*

When $0 < M^2 < 1/\gamma$ the variation $\hat{u}(\hat{T})$ in (37) is qualitatively like that in figure 3. The branch of (37) corresponding to the upper sign is used to describe the increase in speed from the initial point $\hat{T} = 1$ until the critical temperature

$$\hat{T}_c = 1 + \frac{1}{\alpha} = \frac{(1+f)^2}{4f}, \quad f = \gamma M^2 \tag{38a}$$

when

$$\hat{u}_c = (1+f)/2f. \tag{38b}$$

Thereafter the lower-sign branch is used to describe the further acceleration of the flow with declining temperature. The corresponding pressure and local Mach number ($M^2 = M^2\hat{u}^2/\hat{T}$) are given in figures 4 and 5 respectively. In the latter it should be noted that the critical value $M_c^2 = 1/\gamma$. These results show quite specifically that the compressibility of the gas prevents the temperature from rising above T_c. In figure 6 the critical temperature is given as a function of M when $\gamma = 1.4$. For $0.55 \lesssim M \lesssim 1.3$ there are very severe limitations on the maximum temperature rise in the system relative, say, to the adiabatic flame temperature $\hat{T}_{ad} = 1 + h$ when $h = O(1)$. For a wide range of M-values $\hat{T}_c < \hat{T}_{ad}$ for typical values of h.

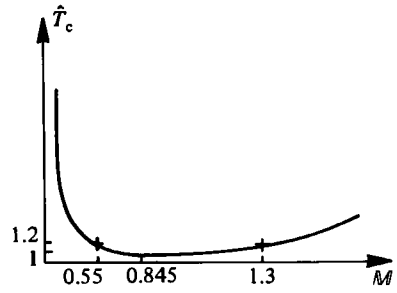

FIGURE 6. Critical temperature as a function of M for $\gamma = 1.4$.

M	$\hat{T}_c$	$\hat{T}_{CJ}$	h_c	h_{CJ}
0.32	2.32	2.26	1.63	1.69
0.55	1.20	1.17	0.31	0.34
0.71	1.03	1.00	0.08	0.104
0.84	1.00	0.97	0.003	0.027
1.05	1.05	1.02	−0.023	0.002
1.14	1.09	1.06	−0.012	0.014
1.22	1.14	1.11	0.007	0.035
1.34	1.23	1.20	0.045	0.074
1.41	1.29	1.25	0.073	0.104
2.00	1.95	1.89	0.422	0.469
2.45	2.63	2.56	0.805	0.868

TABLE 2. Critical parameter values and Chapman–Jouguet parameter values

At the critical point defined by (38) the reactant concentration in (36) can be written as

$$h\hat{y}_c = h - h_c, \quad h_c \equiv T_c - 1 + \tfrac{1}{2}(\gamma-1)M^2(u_c^2-1) > 0, \quad M^2 < 1/\gamma. \tag{39}$$

Typical values of h_c are given in table 2. The critical point concentration $\hat{y}_c$ represents the fuel remaining when the system temperature reaches the critical (in fact maximum possible) value. When $h < h_c$, $\hat{y}_c < 0$ which is physically unacceptable. In this case $y \to 0$ on the upper-sign branch of the curves in figures 3–5 for $\hat{T} < \hat{T}_c$ and $\hat{u} < \hat{u}_c$. For larger values of the heat-release parameter $h > h_c$, $\hat{y}_c > 0$, implying that $y \to 0$ on the lower-sign branch in figure 3 where $\hat{T} < \hat{T}_c$ but $\hat{u} > \hat{u}_c$. When $\hat{y} \to 0$ (36) and (37) can be combined to show that the system temperature approaches

$$\left.\begin{aligned} \hat{T}(\hat{y}=0) = 1 + \frac{\gamma(\gamma-1)}{(\gamma+1)^2}(1-M^2)\frac{1+f}{f}\left[\frac{1-\gamma f}{(\gamma-1)(1+f)}\frac{h}{h_{CJ}} - \left(\frac{1-h}{h_{CJ}}\right) + \left(\frac{1-h}{h_{CJ}}\right)^{\frac{1}{2}}\right], \\ h_{CJ} = \frac{(1-M^2)^2}{2(\gamma+1)M^2}, \quad f = \gamma M^2, \end{aligned}\right\} \tag{40}$$

where h_{CJ} represents the largest allowable value of the heat-addition parameter.† When $h = h_{CJ} > h_c$ the corresponding temperature is

$$\hat{T}_{CJ}(\hat{y}=0) = \left[\frac{1+\gamma M^2}{(\gamma+1)M}\right]^2 = \frac{4\gamma}{(\gamma+1)^2}\hat{T}_c, \tag{41}$$

† Actually h_{CJ} is influenced by the value of the initial strain rate and rate of heat loss to the holder; since both of these quantities are exponentially small they are neglected in (40).

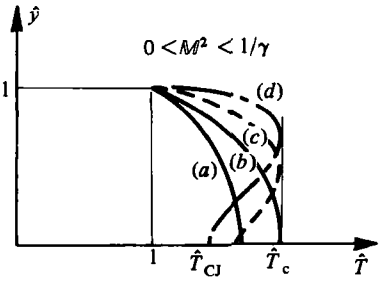

FIGURE 7

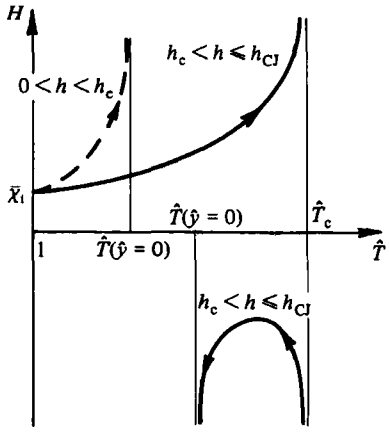

FIGURE 8

FIGURE 7. Reactant concentration as a function of temperature: (*a*) $0 < h < h_c$; (*b*) $h = h_c$; (*c*) $h_c < h < h_{CJ}$; (*d*) $h = h_{CJ}$.

FIGURE 8. H as a function of T. The dashed line is qualitatively correct for $M^2 > 1$ as well.

where $\hat{T}_{CJ} < \hat{T}_c$ for $\gamma > 1$, while the Mach number is

$$M^2(\hat{T}_{CJ}) = M^2\hat{u}^2(\hat{T}_{CJ})/\hat{T}_{CJ} \to 1-. \tag{42}$$

This means that a Chapman–Jouguet condition is approached in the rapid-combustion zone as $\hat{y} \to 0$ if $h = h_{CJ} > h_c$. In contrast, when $h < h_{CJ}$ the local Mach number will be less than unity as $\hat{y} \to 0$.

Typical results for fuel consumption with temperature variation are given in figure 7. When $h < h_c$ the upper-sign branch of (36) is used to find curve (*a*). In this case $1 < \hat{T}(\hat{y} = 0) < \hat{T}_c$. Curve (*b*) corresponds to the special case $h = h_c$. More significant heat addition, $h_c < h < h_{CJ}$, is represented by the curve (*c*), where the critical temperature is attained and $\hat{y}_c > 0$. Further decline in the fuel concentration takes place with a dropping temperature. If $h = h_{CJ}$ the process is described by curve (*d*), which demonstrates that as the fuel vanishes the local Mach number approaches unity from below because the temperature approaches $\hat{T}_{CJ}$. The Chapman–Jouguet condition is observed to occur for a given value of M when just the right amount of heat is generated as all the fuel (at least the lowest approximation thereof) is consumed. If $h < h_{CJ}$ the final temperature will be somewhere between 1 and $\hat{T}_c$ while $M^2 < 1$.

Typical values of h_{CJ} and $\hat{T}_{CJ}$ are given in table 2 for $\gamma = 1.4$. Except at rather small initial Mach numbers the maximum amount of heat that can be added to a steady-state flow is limited. It is noted from (41) that $\hat{T}_{CJ} = 0.972\hat{T}_c$ when $\gamma = 1.4$. This means that in the case $\hat{y}_c > 0$ there will be only a small temperature drop in the system subsequent to the maximum value $\hat{T}_c$. In contrast, the flow acceleration is more substantial because $M_c^2 = 1/\gamma$ while $1/\gamma < M^2 \leqslant M^2(T_{CJ}) = 1$.

In summary then, the subsonic flow is characterized by flow acceleration as the fuel is consumed. If $h < h_c$ the temperature increases monotonically as well. Should the heat addition be sufficiently large, $h_c < h < h_{CJ}$, the temperature increases to $\hat{T}_c$ and then declines slightly to $\hat{T}(\hat{y} = 0)$. The local Mach number will approach unity only when $h = h_{CJ}$.

The value of $\hat{T}^*$ defined in (32) is found from (40) when $h < h_c$. In all other cases

the maximum value of $\hat{T}^* = T_c$. It should be noted from table 2 that when $\hat{T}^*$ is close to unity the β-limitation in (33*b*) is not very severe.

The reduction of the full energy equation (31) to the algebraic formula for $H(\hat{T})$ in (35*a*) is a gratifying by-product of the nonlinear transformation (30). A qualitative description of H is given in figure 8 for the subsonic problem. When $h < h_c$ (35*a*), (36) and (37) can be used to show that the dashed line describes the function. The singularity occurs when $\hat{y} \to 0$ prior to reaching $\hat{T}_c$. In contrast, when $h_c < h \leqslant h_{CJ}$ the functional behaviour is given by the solid line. The first singularity is caused by $(\hat{u}^2)' \equiv \mathrm{d}\hat{u}^2/\mathrm{d}\hat{T}$ becoming unbounded at $\hat{T}_c$ while $\hat{y} \to 0$. The curve reappears in the lower half-plane, reaches a negative maximum and then becomes singular again as $\hat{y} \to 0$. When $h = h_{CJ}$, the factor in brackets in (35*a*) approaches zero as well, but at a slower rate than $\hat{y}$ as $\hat{T} \to \hat{T}_{CJ}$. As a result $H \to -\infty$.

The bracketed factor in (35*a*) is recognized as the temperature derivative of the stagnation temperature

$$\hat{T}_s = \int_1^{\hat{T}} C_p \, \mathrm{d}\sigma + \tfrac{1}{2}(\gamma - 1)\, \mathscr{M}^2 \hat{u}^2.$$

When $H > 0$, $\hat{T}_s$ increases with temperature and in fact with $\bar{\chi}$, given the nature of (30). In the cases $h_c < h \leqslant h_{CJ}$, once the critical point is passed, then $H < 0$, implying that $\hat{T}_s$ decreases with increasing $\hat{T}$. However, the temperature is in fact a decreasing function of $\bar{\chi}$ once $\hat{T}_c$ is achieved because the flow continues to accelerate as the temperature drops. Since the temperature movement is negative $\hat{T}_s$ continues to increase with $\hat{T}_s'(\hat{T}) < 0$. In this sense the stagnation temperature increases monotonically for all possible values of h (cf. Clarke 1983*b*).

The approximations used to derive (35) are not valid when $\epsilon H'(\hat{T}) = O(H)$. This non-uniformity will arise when either of the singularity types in figure 8 are encountered. These singularities must be explored in detail in order to proceed further downstream in the reaction event.

5.2. *Subsonic singularities*

When the singularity generated by vanishing reactant is approached, the terms on the right-hand side of (35*a*) other than $\hat{y}$ have well-defined asymptotes for $h < h_{CJ}$. It follows that $H \sim 1/\hat{y}$ and $\hat{y}^2 H' \sim \hat{y}'$. The derivative $\hat{y}' = O(1)$ when $y \to 0$ according to (35*b*). Then $\epsilon H' = O(H)$ when $\hat{y} = O(\epsilon)$. As a result, when the singularity is approached $H = O(1/\epsilon)$ and $\hat{T} \sim \hat{T}(\hat{y} = 0) + O(\epsilon)$, as can be ascertained from (36) and (40). Similarly $(\hat{p}, \hat{u}) \sim (\hat{p}, \hat{u})\,(\hat{y} = 0) + O(\epsilon)$.

The Chapman–Jouguet case $h = h_{CJ}$ is slightly different because, as $\hat{y} \to 0$, $\hat{y}' \to 0$ as well. A Taylor-series analysis of the singularity can be used to show that $H \sim 1/y^{\frac{1}{2}}$ and that $H' \sim 1/\hat{y}$. Then $\epsilon H' = O(H)$ when

$$\hat{y} = O(\epsilon^2), \quad H = O(1/\epsilon) \quad \text{and} \quad (\hat{T}, \hat{p}, \hat{u}) - (\hat{T}_M, \hat{p}_M, \hat{u}_M) = O(\epsilon).$$

The fuel concentration near the singularity is noted to be an order of magnitude smaller than that for $h < h_{CJ}$. This suggests that a Chapman–Jouguet rapid-reaction zone is a maximally efficient fuel consumer.

The other type of singularity in H, near the critical point, is associated with the properties of $(u^2)'$ because the other factors have well-defined asymptotes. The derivative of (37) can be used to show that

$$\lim_{T \to T_c} H \sim [1 - \alpha(\hat{T} - 1)]^{-\frac{1}{2}},$$

while

$$\lim_{T \to T_c} H' \sim [1 - \alpha(T - 1)]^{-\frac{3}{2}}.$$

The non-uniformity occurs when $\epsilon H' = O(H)$, which implies that $\hat{T} \sim \hat{T}_c + O(\epsilon)$ and $H = O(\epsilon^{-\frac{1}{2}})$. It follows from (37) and (35) that $(\hat{p}, \hat{u}) \sim (\hat{p}_c, \hat{u}_c) + O(\epsilon^{\frac{1}{2}})$, where $\hat{p}_c = 1 - \hat{u}_c$.

In the case of a system for which $h < h_c$ only the first type of singularity will be encountered. However, when $h > h_c$ the second singularity is encountered first in the neighbourhood of the critical point where $\hat{y}_c > 0$. The first type of singularity occurs subsequently when the reactant is finally consumed.

It is convenient at this point to demonstrate that a uniformly valid solution can be constructed in the neighbourhood of the critical point which connects the solutions on the upper- and lower-sign branches of figures 3–5 and which provides the missing part of the H-solution in figure 8. For this purpose we employ (31) and the transformations

$$\hat{T} = \hat{T}_c - \epsilon\tau, \quad J(\tau) = \epsilon^{\frac{1}{2}} H, \quad \tau > 0, \tag{43a,b}$$

which are suggested by the nature of the singularities discussed previously. Equation (37), which remains valid in the limit $\epsilon \to 0$, τ fixed, because (35*c–e*) are appropriate limiting equations, can be used to show that

$$\hat{u} = \hat{u}_c \left[1 \mp \frac{1-f}{1+f} \alpha \tau^{\frac{1}{2}} \epsilon^{\frac{1}{2}} \right]. \tag{44}$$

Then (31), (35*c–e*), (43) and (44) can be combined to find the lowest-order approximation to the equation for $J(\tau)$:

$$J'(\tau) + \hat{T}_c^{-2} J = \pm K \tau^{-\frac{1}{2}}, \quad K = \frac{(\gamma-1)\,\mathscr{M}^2 \hat{u}_c^3\, \alpha^{\frac{1}{2}} (1-f)}{2h\hat{y}_c (1+f)} > 0. \tag{45}$$

The analogous matching condition is

$$J(\tau \to \infty) \sim K \hat{T}_c^2\, \tau^{-\frac{1}{2}}. \tag{46}$$

Equation (45) describes a balance between reactive heat addition and the compressibility effect represented by the non-homogeneous term. Convection is suppressed here to lowest order. The general solution written as

$$J = J(0)\, \mathrm{e}^{-\omega\tau} \pm K\, \mathrm{e}^{-\omega\tau} \int_0^\tau \mathrm{e}^{\omega\sigma}\, \sigma^{-\frac{1}{2}}\, \mathrm{d}\sigma, \quad \omega = \hat{T}_c^{-2}, \tag{47}$$

satisfies (46) when the upper sign is used, without determining the integration constant $J(0)$ that multiplies the homogeneous solution to (45). In fact the exponential decay with respect to τ implies that one would need a term that is exponentially small with respect to the parameter $\epsilon \to 0$ in order to carry out the matching for $J(0)$. The most obvious source of such a term is the neglected transport terms in (31). Given the form of the conduction term in (31) it is apparent that the H-expansion would eventually have a term

$$O\left(\frac{\beta(\epsilon)}{\epsilon H(\hat{T})} \exp\left[\frac{1}{\epsilon} \left(1 - \frac{1}{\hat{T}} \right) \right] \right).$$

In the limit $\hat{T} \to \hat{T}_c$ this would give

$$O\left(\frac{\beta \tau^{\frac{1}{2}}}{\epsilon^{\frac{1}{2}}} \exp\left[\frac{1}{\epsilon} \left(1 - \frac{1}{\hat{T}_c} \right) - \omega\tau \right] \right) \tag{48}$$

if (43*a*) was employed. Given the condition in (32), the matching required by (43*b*) shows that the first term in (47) is of a far larger magnitude than that in (48). It follows

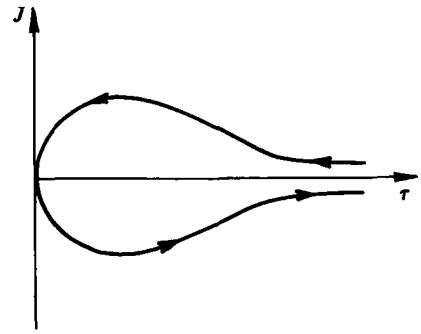

FIGURE 9. J as a function of the temperature perturbation τ. The arrow points in the direction of increasing downstream distance.

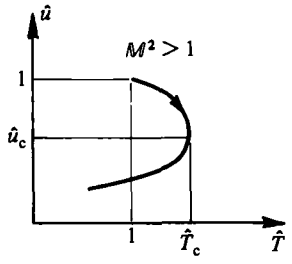

FIGURE 10

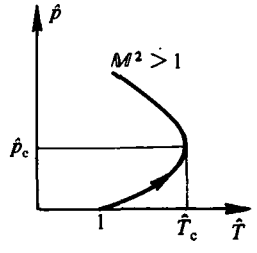

FIGURE 11

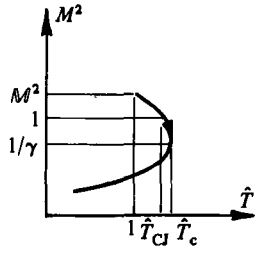

FIGURE 12

FIGURE 10. Flow speed as a function of temperature.

FIGURE 11. Pressure difference as a function of temperature.

FIGURE 12. M^2 as a function of temperature.

that $J(0) = 0$. A qualitative description of $J(\tau)$ is given in figure 9, where the arrow points in the direction of flow. The first location $J' = 0$, on the upper-sign branch of (47), corresponds to a maximum in J and thus H as well. As $\tau \to 0$, $J \to 0+$ so that $H \to 0$ and $\bar{\chi} \to \bar{\chi}_1$, meaning that the ignition delay distance has actually been reached. Subsequently the lower-sign branch is used to describe the function behaviour. There is a subsequent minimum to J, and thus H, followed by an asymptotic approach to zero like $-\tau^{-\frac{1}{2}}$ for $\tau \to \infty$.

The $J(\tau)-$ solution provides the transition in the H-solution in figure 8 from the upper-sign branch (upper half-plane) to the lower-sign branch (lower half-plane) near $\hat{T}_c$. This transitional process occurs over the lengthscale

$$|\bar{\chi} - \bar{\chi}_1| = O\left(\epsilon^{-\frac{1}{2}} \exp\left[-\frac{1}{\epsilon}\left(1 - \frac{1}{\hat{T}_c}\right)\right]\right),$$

a small fraction of the thickness of the complete rapid-combustion zone, which may be found by combining (30) and (43).

5.3. *Supersonic initial conditions*

The deceleration of a supersonic flow by chemical heat-addition is described qualitatively in figures 10–12. Once again the upper-sign branch is used from the initial to the critical point. In contrast to the subsonic case, however, the latter can never be reached because the reactant is always consumed for $1 \leqslant M < M$ while $M_c^2 < 1$. A study of the properties of (40) shows that $1 \leqslant \hat{T}(\hat{y} = 0) \leqslant \hat{T}_{CJ}$. When

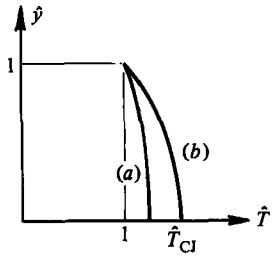

FIGURE 13. Reactant consumption as a function of temperature.

$h = h_{CJ}$ the value of the temperature at which $\hat{y} = 0$ is maximized is $\hat{T}_{CJ}$, implying that the local Mach number is unity. Once again the Chapman–Jouguet condition is attained for a given value of $\mathcal{M}$ and hence h_{CJ}, when the lowest approximation to the reactant concentration vanishes. If, for a given $\mathcal{M}$, $h < h_{CJ}$ then the final Mach number will be supersonic.

The reactant consumption with temperature variation is shown in figure 13. Curve (*a*) describes the process when $0 < h < h_{CJ}$, while the case $h = h_{CJ}$ is given by (*b*).

When $\mathcal{M} > 1$ the qualitative behaviour of the H-function in (35*a*) is given by the dashed line in figure 8 for $0 < h \leqslant h_{CJ}$. The singularity in the H-function when $\hat{y} \to 0$ is like that in the subsonic example and need not be discussed again.

6. The transitional process

The rapid-combustion process is characterized by significant changes in temperature, pressure, speed and reactant concentration. When $\hat{y} = O(\epsilon)$, or $\hat{y} = O(\epsilon^2)$ for $h = h_{CJ}$, and $|H| = O(1/\epsilon)$ the approximations used to derive the basic approximations in (35) fail and one must find another solution which describes the subsequent transition toward the final equilibrium state. This transitional solution must be constructed separately for the situations in which $H \to \infty$ when $\bar{\chi} < \bar{\chi}_i$ and when $H \to -\infty$ for $\bar{\chi} > \bar{\chi}_i$.

6.1. *The case* $H \to \infty$

When the initial speed is subsonic and $0 < h < h_c$ or supersonic with $0 < h < h_{CJ}$ the results of §5 imply that the variables in the transitional solution can be written as

$$(\hat{T}, \hat{p}, \hat{u}) = (\hat{T}_0, \hat{p}_0, \hat{u}_0) + \epsilon(-\tilde{\theta}, \tilde{p}, \tilde{u}), \quad \hat{y} = \epsilon\tilde{y}, \tag{49a,b}$$

$$\bar{\chi}_i - \bar{\chi} = \mu(\epsilon)\,\xi, \quad \mu(\epsilon) = \frac{1}{\epsilon}\exp\left[-\frac{1}{\epsilon}\left(1 - \frac{1}{\hat{T}_0}\right)\right], \tag{49c,d}$$

where the zero subscript refers to values of the rapid combustion zone variables when the associated reactant concentration is zero. For example $\hat{T}_0 \equiv \hat{T}(\hat{y} = 0)$ as in (40). The negative sign is used with $\tilde{\theta}$ because $\hat{T}_0$ is approached from below. If (49) is used in (1) and the limit $\epsilon \to 0$, ξ fixed, is applied, then the lowest-order system is given by

$$\tilde{y}' = \frac{1}{\hat{u}_0}\tilde{y}\,e^{-\tilde{\theta}/\hat{T}_0^2}, \quad -\tilde{\theta} = f\hat{u}_0\tilde{p} + (1 + f\tilde{p}_0)\,\tilde{u}, \tag{50a,b}$$

$$\tilde{\theta}' = \frac{h}{\hat{u}_0}\tilde{y}\,e^{-\tilde{\theta}/\hat{T}_0^2} - \frac{(\gamma-1)f\hat{u}_0\tilde{p}'}{\gamma}, \quad \tilde{p} = -\tilde{u}, \tag{50c,d}$$

where primes denote ξ-derivatives and $f = \gamma \mathscr{M}^2$. These equations are once again devoid of any transport effects. The matching conditions for $\tilde{\theta}(\xi \to \infty)$ can be obtained by relating the behaviour of $H(\hat{T} \to \hat{T}_0)$ and ξ through (30) and (49*c*). It follows that

$$\lim_{\tilde{\theta} \to \infty} \hat{u}_0 \frac{\mathrm{e}^{\tilde{\theta}/\hat{T}_0^2}}{\tilde{\theta}/\hat{T}_0^2}(1 + O(\tilde{\theta}^{-1}) \sim \xi \tag{51}$$

describes the $\tilde{\theta}$-properties. In deriving (51) one must account for the possible effects of higher-order terms in the asymptotic expansion for $H(\hat{T}; \epsilon)$. Similarly (49*b*) and (36) can be used to show that

$$\lim_{\xi \to \infty} h\tilde{y} \sim h(1 + (\gamma - 1)\mathscr{M}^2 u_0^{2\prime})\,\tilde{\theta} + \hat{y}_{10}, \tag{52}$$

where $\hat{y}_{10}$ represents the constant limiting function form of the $O(\epsilon)$ perturbation for $\hat{y}$ (e.g. $\hat{y} \sim \hat{y}_0 + \epsilon \hat{y}_1 + \ldots$) in the rapid-combustion zone. This behaviour can be rationalized by considering the higher-order analogue of (35*b*).

Equation (50) can be reduced to

$$\tilde{\theta}' = -\hat{\rho}_0(\tilde{\theta}_\infty - \tilde{\theta})\,\mathrm{e}^{-\tilde{\theta}/\hat{T}_0^2}, \tag{53a}$$

$$h\tilde{y} = \tilde{k}(\tilde{\theta}_\infty - \tilde{\theta}), \quad \tilde{k} = \frac{1 + f - \dfrac{1+\gamma}{\gamma} f\hat{u}_0}{2f\hat{u}_0 - (1+f)}, \quad \tilde{\theta}_\infty = \frac{\hat{y}_{10}}{\tilde{k}}, \tag{53b}$$

where $\tilde{\theta}_\infty$ represents the asymptotic value of $\tilde{\theta}$ far downstream ($\xi \to -\infty$). An explicit evaluation would require calculating the entire first-order correction to the rapid-combustion process, which will not be carried out here.

The formal solution to (53*a*) can be written as

$$\int_1^\sigma \frac{\mathrm{e}^{-s}\,\mathrm{d}s}{s} = \frac{\mathrm{e}^{\tilde{\theta}_\infty/\hat{T}_0^2}}{\hat{u}_0}(\xi + \tilde{k}), \quad \sigma = \frac{\tilde{\theta}_\infty - \tilde{\theta}}{\hat{T}_0^2}, \tag{54}$$

which will satisfy the condition in (51) if

$$\tilde{k} = \hat{u}_0\,\mathrm{e}^{\tilde{\theta}_\infty/\hat{T}_0^2} \int_1^\infty \frac{\mathrm{e}^{-s}\,\mathrm{d}s}{s}. \tag{55}$$

Most significantly (54) shows that

$$\lim_{\xi \to -\infty} \sigma \sim \exp\left(-\left[\frac{\mathrm{e}^{-\tilde{\theta}_\infty/\hat{T}_0^2}}{\hat{u}_0}\right](-\xi)\right), \tag{56}$$

meaning that the asymptotic temperature-perturbation value $-\tilde{\theta}_\infty$ is approached exponentially fast. It follows from (53*b*) that the reactant concentration $\epsilon\tilde{y} \to 0$ exponentially fast as $\xi \to -\infty$.

The perturbation solutions for $\tilde{p}$ and $\tilde{u}$ can be found easily from (50*b*,*d*) once $\tilde{\theta}$ is known from (54).

The transitional solution describes the relaxation of the system to a nearly equilibrium state in which the reactant concentration is becoming very small. In fact, if the related thermal-explosion theory is a guide (Kassoy 1977), there will be a succession of subsequent regions in which exponentially small amounts of fuel are consumed. In these regions transport effects are once again of interest because they too are exponentially small with respect to the parameter $\epsilon \to 0$.

The ultimate final state can of course be calculated from (7).

6.2. *The case* $H \to -\infty$

When $0 < \mathcal{M}^2 < 1/\gamma$ and $h_c < h < h_{CJ}$ the H-function is large and negative when $\hat{y} \to 0$. This implies from (30) that the singularity occurs beyond the location of the ignition delay $\bar{\chi}_i$. It is convenient in this case to carry out the solution in terms of the independent variable $\tilde{T}$ and then use (30) to find the spatial dependence. Given the nature of the singularity, the transition-zone variables can be defined by

$$(\hat{u}, \hat{p}) = (\hat{u}_0, \hat{p}_0) + \epsilon(\tilde{u}, \tilde{p}), \quad \hat{y} = \epsilon\tilde{y}, \quad H = \frac{\tilde{L}}{\epsilon}, \tag{57a,b,c}$$

where $\tilde{u}$, $\tilde{p}$, $\tilde{y}$ and $\tilde{L}$ are functions of the independent variable $\tilde{T}$ given by

$$\hat{T} = \hat{T}_0 + \epsilon\tilde{T}. \tag{58}$$

The zero subscript is as defined in §6.1. These variables may be used in (31), the analogous species and momentum equations and (1*e*) to find the lowest-order approximate system

$$1 = \frac{h\tilde{y}}{\hat{u}_0}(\hat{T}_0^{-2}\tilde{L} - \tilde{L}') + (\gamma - 1)\mathcal{M}^2\hat{u}_0\tilde{p}', \tag{59a}$$

$$\tilde{y}' = -\frac{\tilde{y}}{\hat{u}_0}(\hat{T}_0^{-2}\tilde{L} - \tilde{L}'), \tag{59b}$$

$$\tilde{p} = -\tilde{u}, \quad \hat{p}_0 = 1 - \hat{u}_0, \tag{59c}$$

$$\tilde{T} = \hat{u}_0 f\tilde{p} + (1 + \hat{p}_0 f)\tilde{u}, \quad \hat{T}_0' = \hat{u}_0(1 + \hat{p}_0 f), \tag{59d}$$

where primes denote derivatives with respect to $\tilde{T}$. The general solution has the form

$$\tilde{p} = -\tilde{u} = \tilde{a}T, \quad \tilde{a} = (1-f)(1 - \alpha(\hat{T}_0 - 1))^{\frac{1}{2}} > 0, \tag{60a}$$

$$h\tilde{y} = \tilde{b}\tilde{T} - \tilde{C}, \quad \tilde{b} = \frac{(\gamma-1)f\hat{u}_0\tilde{a}}{\gamma} - 1 > 0, \tag{60b}$$

$$\tilde{L} = -\hat{u}_0 \mathrm{e}^{\tilde{T}/\hat{T}_0^2} \int_{\tilde{T}}^{\infty} \mathrm{e}^{-\sigma/\hat{T}_0^2} (\ln\tilde{y})' \, \mathrm{d}\sigma, \tag{60c}$$

where $\tilde{C}$ in (60*b*) is an integration constant. In deriving (60*c*) it has been assumed that $\tilde{L}$ is not exponentially large as $\tilde{T} \to \infty$.

The solution in (60) must be matched with the asymptotic form of the rapid-combustion-zone solutions when $\hat{T} \to \hat{T}_0$ from above. This implies that $\tilde{T} \to \infty$. For example the asymptotic form of the $\tilde{L}$-function, obtained from (60*c*), is

$$\tilde{L}(\tilde{T} \to \infty) \sim -\frac{\hat{u}_0\hat{T}_0^2}{\tilde{T}}\left(1 + O\left(\frac{1}{\tilde{T}}\right)\right).$$

Then (57*c*) and (58) can be used to show that

$$H(\hat{T} \to \hat{T}_0) \sim -\frac{\hat{u}_0\hat{T}_0^2}{\hat{T} - \hat{T}_0}.$$

The direct asymptotic estimate for H, found from (35), (36) and the lower-sign form of (37), is identical, thus verifying the previous assumption on the $\tilde{L}$-behaviour used to find (60*c*). In a similar manner the $\tilde{p}$-, $\tilde{u}$- and $\tilde{y}$-solutions can be matched. It should be noted that $\tilde{C}$ cannot be found without calculating the $O(\epsilon)$ correction to $\hat{y}$ in the rapid-combustion zone and carrying out the appropriate higher-order matching.

Nevertheless (60*b*) shows that when $\tilde{T} = \tilde{C}/\tilde{b}$ the $O(\epsilon)$ fuel concentration defined in (57*b*) vanishes and from (58) shows that $\tilde{T}$ is within an $O(\epsilon)$ value from $\hat{T}_0$. When $\tilde{y} \to 0$ (60*c*) can be used to show that

$$-\tilde{L}(\tilde{y} \to 0) \sim \hat{u}_0 \ln(1/\tilde{y}),$$

which is logarithmically singular. This result can be combined with (30) and (57*c*) to show that

$$\bar{\chi} \sim \bar{\chi}_i + \epsilon^{-1} \exp\left[-\frac{1}{\epsilon}\left(1 - \frac{1}{\hat{T}_0}\right)\right] \ln\left(\frac{1}{\tilde{y}}\right) \hat{u}_0 \, e^{\tilde{C}/\tilde{b}\hat{T}_0^2},$$

which demonstrates that as the fuel is consumed we continue to move downstream away from $\bar{\chi}_i$ (which occurred when the temperature was close to $\hat{T}_c$).

The Chapman–Jouguet case $h = h_{CJ}$ must be treated separately because $\hat{y} = O(\epsilon^2)$ when the rapid-combustion-zone analysis fails. However, the approach is similar to that just concluded. Most notably (57*b*) must be replaced by

$$\hat{y} = \epsilon^2 \tilde{y}, \tag{61a}$$

and

$$(\tilde{u}, \tilde{p}) \sim (\tilde{u}_1, \tilde{p}_1) + \epsilon(\tilde{u}_2, \tilde{p}_2) + \ldots \tag{61b}$$

must be used to find $O(\epsilon^2)$ corrections to $(\hat{u}, \hat{p})$ corresponding to the $O(\epsilon^2)$ fuel-concentration field. Then, proceeding as before, the solutions are found to be

$$\tilde{p}_1 = -\tilde{u}_1 = \frac{(\gamma+1)\tilde{T}}{(f+1)(\gamma-1)}, \tag{62a}$$

$$\tilde{p}_2 = -\tilde{u}_2 = f\left[\frac{\gamma+1}{(f+1)(\gamma-1)}\right]^3 \tilde{T}^2, \tag{62b}$$

$$h_{CJ}\,\tilde{y} = \frac{f}{(f+1)^2} \frac{(\gamma+1)^3}{\gamma(\gamma-1)^2} \frac{\tilde{T}^2}{2} - \tilde{C}, \tag{62c}$$

$$\tilde{L} = -\hat{u}_{CJ} \, e^{\tilde{T}/\hat{T}_{CJ}^2} \int_{\tilde{T}}^{\infty} e^{-\sigma/\hat{T}_{CJ}^2} (\ln \tilde{y})' \, d\sigma, \tag{62d}$$

where $\hat{u}_{CJ}^2 = T_{CJ} M^{-2}$ and $\tilde{C}$ is an integration constant. These solutions can be shown to match with those from the rapid-combustion zone when $\tilde{T} \to \infty$. Here again $\tilde{C}$ cannot be evaluated formally without a higher-order analysis of the rapid-combustion zone. As $\tilde{y} \to 0$, $\tilde{T}$ will approach an $O(1)$ value, implying that as the $O(\epsilon^2)$ fuel is consumed that temperature is within $O(\epsilon)$ of T_{CJ}. Once again $-\tilde{L}$ will have a logarithmic singularity for $\tilde{y} \to 0$, so that downstream motion is preserved in the spatial transformation.

The supersonic Chapman–Jouguet transition-zone solution is quite similar to that completed above for the subsonic flow. In the interest of brevity, and because the solution lacks any novelty, it will not be discussed further.

7. Conclusions

A mathematical model has been developed for a one-dimensional steady high-speed deflagration when a unimolecular decomposition reaction of the Arrhenius type determines the rate of heat addition. The flow evolves from a non-equilibrium origin which represents the exit of an experimental apparatus. This burner configuration permits one to work with a well-posed mathematical system when the kinetics are described in terms of the ordinary Arrhenius rate law. The reactive compressible flow

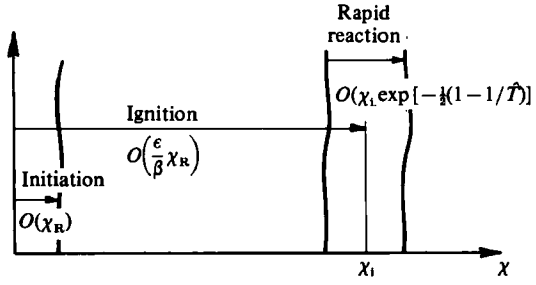

FIGURE 14. The major zone structure, where χ_R is given in (3) and χ_1 in (29).

is studied for arbitrary values of the Lewis and Prandtl numbers, for general variations of viscosity, conductivity and diffusivity and for a temperature-dependent specific heat C_p. A complete solution is obtained in the limit of high activation energy when the shortest possible characteristic reaction time is large with respect to the typical time interval between molecular collisions.

Reaction initiation occurs adjacent to the origin in a region scaled in extent by a modest multiple of the mean free path of the gas. A balance of weak chemical heat-addition and transport effects produce exponentially small, but finite, gradients which can adjust to a wide range of input Mach numbers M. In a subsequent region there is a fundamental balance of convection, reaction and compressibility which leads to a thermal explosion-like ignition process at the dimensional location

$$x_i = \frac{\epsilon(1-M^2)}{(1-\gamma M^2)\,h}[u_1 B^{-1} e^{1/\epsilon}] \tag{63}$$

when $M^2 < \gamma^{-1}$ or $M^2 > 1$. In the former case the result is identical with that found by Erpenbeck (1963) in a study of a subsonic reaction zone downstream of a shock. The term in square brackets represents the distance travelled by a fluid particle moving at the initial speed u_1 during the characteristic initial-reaction time $B^{-1}e^{1/\epsilon}$.

As $x \to x_i -$ a more violent reaction process occurs on a lengthscale short compared with x_i but large compared with x_R in (3). Unlike the previous, induction zone, where $O(\epsilon)$ changes in reactant concentration and temperature occur, there are $O(1)$ changes in each of the physical variables. The rapid-combustion process, determined by a balance of convection, reaction and compressibility, proceeds until the reactant has nearly vanished. Variations in the temperature and speed with distance are determined by the strong interaction between heat addition and compressibility. The latter effect tends to limit the temperature rise in the subsonic case because thermal energy is readily converted to kinetic energy. Since transport properties are of negligible importance in this zone, the basic conservation equations for mass and momentum and the state equation reduce formally to those which describe the variations from one state of local mechanical and thermal equilibrium to another in a one-dimensional compressible flow with heat addition (Williams 1965). However, the energy and reactant-species conservation equations contain Arrhenius kinetic laws which determine the nature of the distributed heat release in the rapid-combustion zone. Thus local states of *chemical* equilibrium (zero reaction rates) do not exist.

The solutions imply that subsonic deflagrations will develop downstream of the initial point for a wide range of downstream pressures, each of which corresponds to exponentially small initial strain rate and temperature gradient. In contrast, a purely supersonic deflagration can exist for a range of downstream pressures only if the

initial gradients take on a set of very specific values. Such a process would be unlikely in practice because the gradient control would be impossible.

The high-speed deflagration described here is generally equivalent to the reaction behind a planar shock in the idealized detonation-wave model. It is well known that the interaction between the shock wave and exothermic processes in the reaction zone lead to a basic flow instability which destroys the one-dimensionality of an initially planar wave (Erpenbeck 1970). The stability properties of the reaction zone will be a profitable area of study in the future.

When the input Mach number M in the burner model is sufficiently large, the flame behaves like a convecting thermal explosion (Clarke 1983*a*). Gradients at the burner are exponentially small with respect to the high-activation-energy parameter limit. They have only the most negligible effect on the global properties of the flame. However, the finiteness of the gradients permits the system to adjust to a wide range of M-values.

The theory of doubly infinite low-speed transport-property-dominated flames (Buckmaster & Ludford 1982) predicts a unique propagation speed when the up- and downstream states are in perfect equilibrium. If the unburned-gas state admits very small but finite gradients, then Johnson (1963) has demonstrated that the uniqueness of the flame speed is lost. Similarly, for low-speed burner-attached flames, finite gradients at the origin permit the system to adjust to a wide range of input mass-flow rates. In effect, the flame-propagation speed can take a wide range of values.

The doubly infinite field models of high-speed flames given by Kapila *et al.* (1983) and Stewart & Ludford (1983) predict unique flame speeds as a function of an ignition temperature, thought of as a material property of the reactant, at which the upstream chemical reaction is suddenly initiated. Although the concept of an ignition temperature was suggested by von Kármán & Millan (1953), there is no evidence in the literature to suggest that it can be considered to be a material property, independent of an apparatus. In this respect it is our opinion that the ignition-temperature concept is not really helpful in developing a completely defined model of a flame. Further, it is our belief that the 'finiteness' of any real combustion experiment must be accounted for in a physically viable mathematical model of the system. This requirement will preclude the possibility of perfectly-equilibrium end states. The formulation of the present model emphasizes that, so long as the tiniest finite gradients are permitted at a specific location upstream of the flame, a normal Arrhenius kinetic model can be used to describe the spatial evolution of a reaction from any chosen initial temperature. In our view these are appealing physical attributes.

Finally, it should be mentioned that the reaction model employed in the analysis provided the least complex equation system with distributed heat release. An extension of the study to include bimolecular initiation reactions, a model of chain branching, a termination reaction and an equilibrium dissociation–recombination step is desirable, although algebraically complicated (Birkan & Kassoy 1983).

This research was supported by a Faculty Fellowship from the University of Colorado, by a visiting Fellowship from the Science and Engineering Research Council of the United Kingdom and by a grant from the U.S. Army Research Office DAAG 29-83-K-0069. It was completed while DRK was enjoying the hospitality of the School of Mathematics and Physics at the University of East Anglia.

REFERENCES

ADAMSON, T. C. 1960 *Phys. Fluids* **3**, 706.

BIRKAN, M. & KASSOY, D. R. 1983 *Combust. Sci. Tech.* **33**, 125.

BOWEN, J. R. 1967 *Phys. Fluids* **10**, 290.

BRADLEY, J. N. 1962 *Shock Waves in Chemistry and Physics*. Methuen.

BUCKMASTER, J. D. & LUDFORD, G. S. S. 1982 *Theory of Laminar Flames*. Cambridge University Press.

BUSH, W. B. & FENDELL, F. E. 1970 *Combust. Sci. Tech.* **1**, 421.

BUSH, W. B. & FENDELL, F. E. 1971 *Combust. Sci. Tech.* **2**, 271.

CARRIER, G. F., FENDELL, F. E. & BUSH, W. B. 1978 *Combust. Sci. Tech.* **18**, 33.

CLARKE, J. F. 1983*a* *Combust. Flame* **50**, 125.

CLARKE, J. F. 1983*b* *J. Fluid Mech.* **136**, 139.

CLARKE, J. F. & MCINTOSH, A. C. 1980 *Proc. R. Soc. Lond.* A **372**, 367.

COURANT, R. & FRIEDRICHS, K. O. 1948 *Supersonic Flow and Shock Waves*. Interscience.

CURTISS, C. F., HIRSCHFELDER, J. O. & BARNETT, M. P. 1959 *J. Chem. Phys.* **30**, 470.

DUFF, R. E. 1978 *J. Chem. Phys.* **28**, 1193.

ERPENBECK, J. J. 1962*a* *Phys. Fluids* **5**, 604.

ERPENBECK, J. J. 1962*b* *Phys. Fluids* **5**, 1181.

ERPENBECK, J. J. 1963 In *Proc. 9th Symp. (Intl) on Combustion*, p. 442. The Combustion Institute.

ERPENBECK, J. J. 1964 *Phys. Fluids* **7**, 684.

ERPENBECK, J. J. 1967 *Phys. Fluids* **10**, 274.

ERPENBECK, J. J. 1970 *Phys. Fluids* **13**, 2007.

FICKETT, W. & DAVIS, W. C. 1979 *Detonation*. University of California Press.

HIRSCHFELDER, J. O. & CURTISS, C. F. 1949 *J. Chem. Phys.* **17**, 1076.

HIRSCHFELDER, J. O. & CURTISS, C. F. 1958 *J. Chem. Phys.* **28**, 1130.

JOHNSON, W. E. 1963 *Arch. Rat. Mech. Anal.* **13**, 46.

KAPILA, A. K., MATKOWSKY, B. J. & VAN HARTEN, A. 1983 *SIAM J. Appl. Maths* **43**, 491.

KÁRMÁN, T. VON & MILLÁN, G. 1953 In *Anniversary Volume on Applied Mechanics Dedicated to C. B. Bienzo*, p. 58. Haarlem, N. V. de Technisch Uitgeverij H. Stan.

KASSOY, D. R. 1975 *Q. J. Mech. Appl. Maths* **28**, 63.

KASSOY, D. R. 1977 *Q. J. Mech. Appl. Maths* **30**, 71.

KOUMOUTSOS, N. G. & KOVITZ, A. A. 1963 *Phys. Fluids* **6**, 1007.

LANDAU, L. D. & LIFSHITZ, E. M. 1959 *Fluid Mechanics*. Pergamon.

LINDER, B., CURTISS, C. F. & HIRSCHFELDER, J. O. 1958 *J. Chem. Phys.* **28**, 1147.

LU, G. C. & LUDFORD, G. S. S. 1982 *SIAM J. Appl. Maths* **42**, 625.

NICHOLLS, J. A. 1963 In *Proc. 9th Symp. (Intl) on Combustion*, p. 488. The Combustion Institute.

SEMENOV, N. N. 1928 *Z. Phys.* **48**, 571.

SHAPIRO, A. 1954 *The Dynamics and Thermodynamics of Compressible Fluids Flow*, vol. I. Ronald.

STEWART, D. S. & LUDFORD, G. S. S. 1983 *J. Méc.* **3**, 463.

TARVER, C. M. 1982 *Combust. Flame* **46**, 111.

WILLIAMS, F. A. 1965 *Combustion Theory*. Addison Wesley.

WOOD, W. W. 1961 *Phys. Fluids* **4**, 46.

WOOD, W. W. & SALSBURG, Z. W. 1960 *Phys. Fluids* **3**, 549.